RESEARCH REPORT

VTT-R-03074-09

Steel Solutions for the seismic retrofit and upgrade of existing constructions

Upgrading/retrofitting proposals for masonry structure using steel solutions

Authors: Ludovic Fülöp

Confidentiality: Confidential

Public after closing the project (July 2010).

Report's title	
Upgrading/retrofitting proposals for masonry structure using steel solutions	
Customer, contact person, address Commission of the European Communities	Order reference RFS-PR-06054
Project name Steel Solutions for Seismic Retrofit and Upgrade of Existing Constructions	Project number/Short name 12597/STEELRETRO
Author(s) Ludovic Fülöp	Pages 29 p.
Keywords masonry structure, pushover analysis, earthquake performance	Report identification code VTT-R-03074-09

Summary

This document is part of the project STEELRETRO, Work Package 3. One task of the work package was to evaluate the earthquake performance of a masonry building, and to propose rehabilitation and retrofitting solutions in order to improve it. The results of this task are reported in this document. The building under investigation was the "Masonry benchmark building" proposed within the STEELRETRO project.

Finite Element Modeling of the building is carried out in this work, evaluating the earthquake performance using the pushover methodology. The proposed rehabilitation techniques are classified based on their technical performance.

Public after closing the project (July 2010).

Confidentiality	Confidential

Espoo18.1.2010

Written by	Reviewed by	Accepted by
Ludovic Fülöp Senior Research Scientist	Ilkka Hakola Senior Research Scientist	Eila Lehmus Technology Manager

VTT's contact address
P.O. Box 1000, FI-02044 VTT, Finland

Distribution (customer and VTT)

Customer (Partners of RFCS project STEELRETRO):	1 pdf copy
VTT/Register Office:	1 copy

The use of the name of the VTT Technical Research Centre of Finland (VTT) in advertising or publication in part of this report is only permissible with written authorisation from the VTT Technical Research Centre of Finland.

Preface

The report is part of the project STEELRETRO, Work Package 3. The overall aim of the STEELRETRO project is to "*set up steel solutions for the seismic retrofit of existing buildings, furnishing design and construction methodologies, tools for dimensioning of elements and connections as well as for cost estimation*".

Specifically, Work Package 3 aims at analyzing and designing "*steel solutions to retrofit or upgrade vertical systems of existing reinforced concrete building, in terms of strength or stiffness, by means of steel concentric bracing systems, steel eccentric bracing systems or shear steel/composite walls.*" and "*steel solutions to retrofit or upgrade vertical systems of existing masonry building coupling the existing structure with new a steel structure or with a bracing systems.*"

WP 3 also aims at analysis and design of "*steel solutions to retrofit or upgrade vertical systems of existing reinforced concrete building and masonry buildings, in terms of ductility by the application of dissipative steel systems and in particular by eccentric steel bracings, steel shear panels/walls and BRB (buckling restrained brace) systems.*"

Within WP 3, VTT had the role of analyzing "*possible solutions using light gauge steel shear walls*" for the r.c. frame structures; and light-gauge steel solutions both for the masonry building.

This report summarizes the work carried out for the rehabilitation of the benchmark masonry building.

Espoo 18.1.2010

Authors

Contents

Abbreviations

LGS – light gauge steel

FE – finite element

DP – damage plasticity

PGA – peak ground acceleration

PSA –pseudo-spectral acceleration

SD – spectral displacement

FRP – fibber-reinforced polymer

SDOF – single degree of freedom oscillator

1 Introduction

The purpose of this report is to provide data on the efficiency of retrofitting of masonry structures using steel strengthening solutions. Specifically, a “masonry benchmark structure” has been used as application example of the different rehabilitation techniques. The aim was to use advanced analysis methods to (i) determine the weaknesses of the initial structure and (ii) to test the benefits of different rehabilitation and strengthening solutions. One of the focuses of the work is the use of horizontal LGS steel strips as strengthening method. However, this method was applicable only when coupled with other methods (e.g. ensuring diaphragm behavior of floors).

2 Description of the structure

2.1 Geometry

The geometry of the structure was based on the description by Braconi *et al* [1] and is briefly reproduced in Figure 1 and Figure 2.

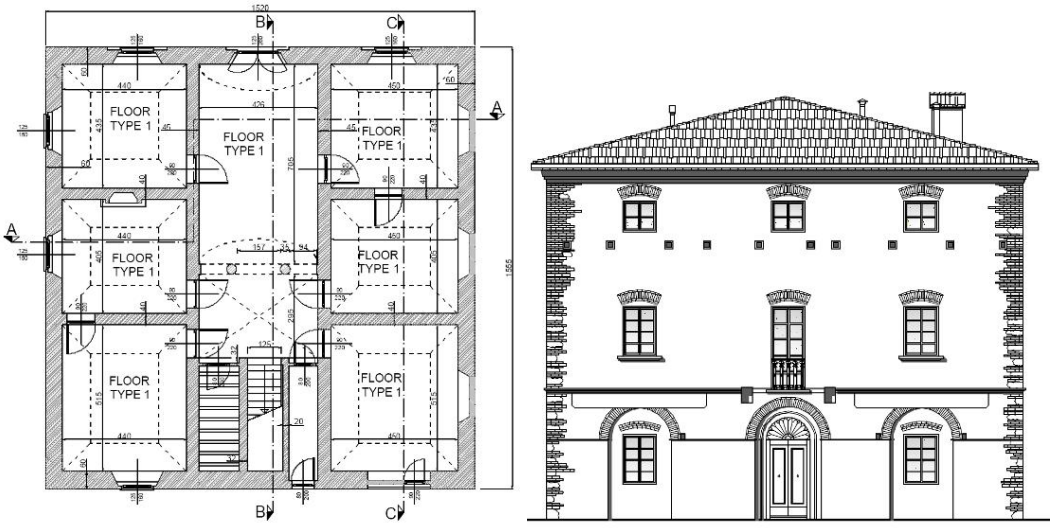

(a) (b)

Figure 1. Ground floor section (a) and selected facade (b) of the building.

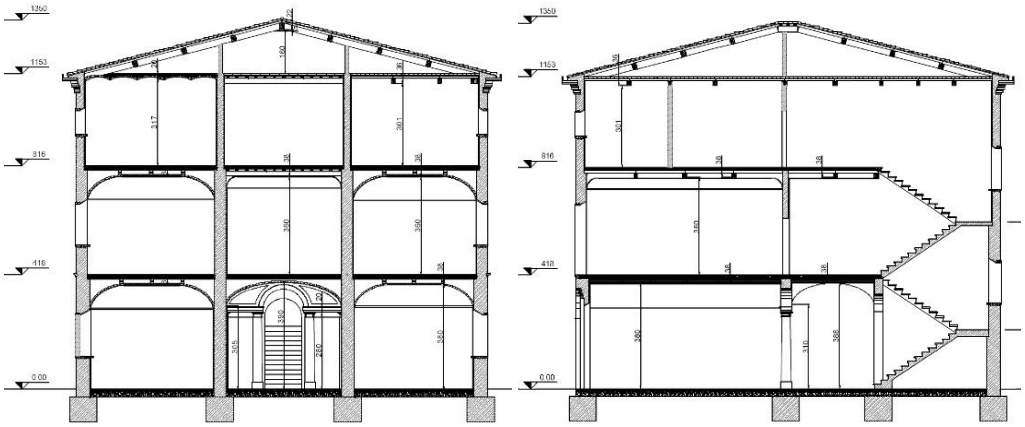

Figure 2. Section A-A and section B-B from Figure 1.

2.2 Materials

The material properties used in the modeling correspond to the ones specified by Braconi *et al* [1]. For all walls the "Stone masonry" specification was utilized. The effect of hollow brick masonry infill walls has been neglected in the modeling. E.g. some windowpanes of the structure have been filled with hollow brick masonry; these were considered empty.

2.3 Loads

Only loads in the seismic combination have been considered in this analysis. A more detailed study on this structure, including other load combinations is reported by Varelis *et al* [2].

2.3.1 Weight, seismic masses

An independent evaluation of the masses has been done independently, and values very close to the ones reported in [2] have been found. In order to maintain compatibility between the results in Varelis *et al* [2] and this report, the masses of the building and the loadings have been following the values reported by Varelis.

According to the evaluation of the loads the structure has a weight distribution presented in Table 1 and Figure 3a. As it can be observed the largest contribution to the weight (i.e. seismic mass), is given by the masonry walls. This implies that the modeling using equivalent horizontal forces at the floor levels (as done is this modeling) can be questionable because the distribution of masses is more uniform along the height of the building. The total seismic mass is 1509 kN.

Table 1. Weight distribution in the masonry building (in N & tons).

	Weight (N)				Mass
	Walls	Floors+ Live load	Total	Total (%)	(t)
Ground floor	4598380	1562440	6160820	40.8	628.0
1st floor	4087460	1225294	5312754	35.2	541.6
2nd floor+Roof	2503860	1121602	3625462	24.0	369.6
Total	11189700	3909336	15099036		1539.1
%	74.1	25.9	100.0		

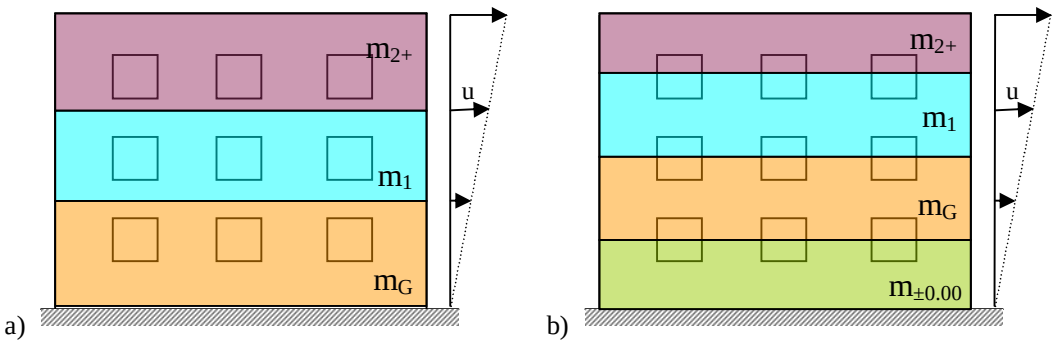

Figure 3. Concentration of masses (a) standard (b) alternative.

2.3.2 Distribution of the seismic loads

In the standard case, masses were concentrated on the structure, to each floor level according to Table 1 (i.e. this is in accordance to Varielis *et al* [2]). Horizontal forces were determined presuming a linear increase of the lateral displacement with the height, according to the procedure from EN 1998 [7] (Figure 4). The resulting horizontal load distribution and the properties of the equivalent SDOF oscillator are presented in Table 2. As presented in the table, horizontal loads were distributed to floor levels in the proportion 23.2% to 1st slab level, 39.1% to 2nd slab level and 37.7% to roof level.

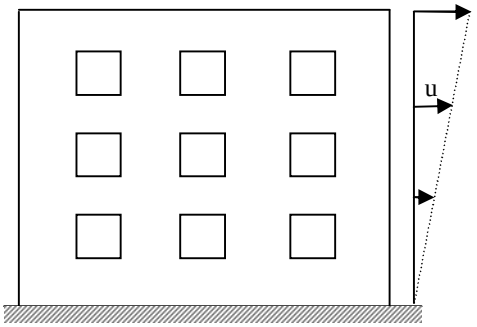

Figure 4. Presumed distribution of lateral displacements with height.

Table 2. Distribution of horizontal loads and properties of the equivalent SDOF (mass distribution according to Figure 3a).

Level	h(m)	m_{sum}(t)	Φ_j	$m_{sum}\cdot\Phi_j$	$m_{sum}\cdot\Phi_j^2$	$h\cdot m_{sum}\cdot\Phi_j$	F_h(%)
G	4.18	628.0	0.36	227.7	82.5	951.7	23.2
1	8.16	541.6	0.71	383.3	271.3	3127.5	39.1
2+R	11.53	369.6	1.00	369.6	369.6	4261.1	37.7
Sum:		1539.1	1	980.5	723.4	8340.3	100.0

"Modal participation factor"	$\Gamma_1 = m^*/(m_j\cdot\Phi_j^2)$	1.36	
Effective modal mass	$M_1^* = (m^*)^2/(m_j*\Phi_j^2)$	1329.10	t
Effective modal height	$h_1*=L_1^{\theta}/L_1^{h}$	8.506	m

An alterative distribution of masses has also been used in the modeling (Figure 3b). In this case, the structure was slightly lighter (because floor mass was evaluated differently); but more importantly, the masses have been concentrated to floors in a different way (Table 3). Compared to the standard distribution the alternative one is generating smaller horizontal demand, because part of the seismic mass is reduced to the ground floor, and therefore does not generate horizontal loads on the structure.

The forces in the alternative distribution and the properties of the equivalent SDOF are, in this case are presented in Table 3. Results obtained with the alternative distribution are not reported in detail in this document, but in §4.2.2, reference will be made to them in order to highlight the sensitivity of the modeling to the adopted horizontal loading pattern.

Table 3. Distribution of horizontal loads and properties of the equivalent SDOF (mass distribution according to Figure 3b).

Level	h(m)	m_{sum}(t)	Φ_j	$m_{sum}\cdot\Phi_j$	$m_{sum}\cdot\Phi_j^2$	$h\cdot m_{sum}\cdot\Phi_j$	F_h(%)
+-0.00	0	234.4	0.00	0.0	0.0	0.0	0.0
G	4.18	567.5	0.36	205.8	74.6	860.1	26.6
1	8.16	447.5	0.71	316.7	224.1	2584.4	41.0
2	11.53	249.8	1.00	249.8	249.8	2880.0	32.3
Sum:	11.53	1499.2	1	772.3	548.5	6324.5	100.0

"Modal participation factor"	$\Gamma_1 = m^*/(m_j\cdot\Phi_j^2)$	1.41	
Effective modal mass	$M_1^* = (m^*)^2/(m_j*\Phi_j^2)$	1087.24	t
Effective modal height	$h_1* = L_1^{\theta}/L_1^{h}$	8.190	m

2.3.3 Magnitude of the seismic loads

The seismic load was considered respecting the recommendations of Varelis *et al* [2]. As a general design target a PGA (a_g) of 0.23g has been considered, with a Type 1 elastic spectrum on Soil B, according to EN 1998 [7]. The value of the damping was ξ = 5% for the design, and the structure was classified as importance Class II [8]. The target elastic spectrum (S_e) is presented in pseudo-spectral acceleration vs. spectral displacement format in Figure 5. Se corresponds to the characteristic value of the seismic action (A_{Ek}) for the ULS check. The design value of the seismic action (A_{Ed}) can be derived from A_{Ek}, by taking into account that: (i) the correction due to the importance class of the building (γ_1=1), (ii) the possibility to reduce base shear with the factor λ=0.85 for buildings with more than 2 levels [7], and $T_1<2\times T_C$=4s and (iii) the possible use of a q factor larger than q=1. In Figure 5, the potential A_{Ed} curves, corresponding to fully elastic behavior (q=1) and the minimal value of the reduction factor (q=1.5), permitted by EN1998 [7] has been plotted.

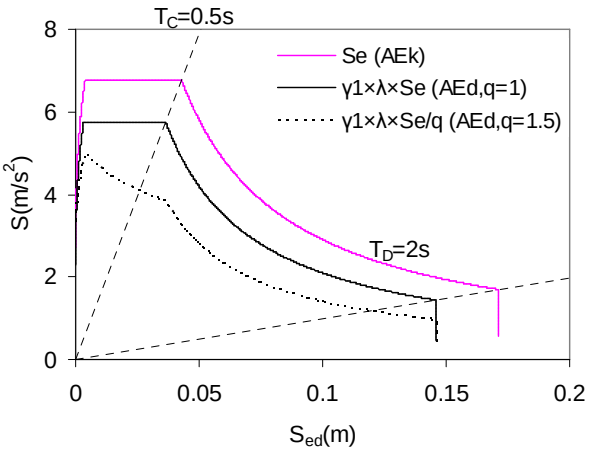

Figure 5. PSA vs. SD format of the elastic target spectra for the design.

In the low period range T < 0.5s, which corresponds to the period of masonry structures, the PSA (A_{Ed}) is at the levels of 5.75 m/s^2. This means that, if fully elastic response and equivalency of the structure with a SDOF system is presumed, the 1539 ton seismic mass would generate ~885 tons of base shear force. F_b = 8855 kN can be used as an indicative value for quick evaluation.

3 Description of the FE model

3D modeling with Finite Element (FE) has been proposed for the structure by Dogariu [3]. This model, developed in ABAQUS has been the basis of the analysis reported here. Several adaptations have been made to the initial FE model, but the geometry is essentially unchanged and the original concrete Damage Plasticity (DP) model proposed by Dogariu [3] has been extensively used.

3.1 Material models used for the analysis

Two material models have been tried for the modeling of the masonry behavior. One was the initial proposal made by Dogariu [3], for the use of the in-built concrete damage plasticity model of ABAQUS. The disadvantage of this model is that it can not handle orthotropic behavior, and therefore is not very well suited for modeling masonry, which has different properties parallel and perpendicular to the bed joint.

The second material model was based on the orthotropic model developed by Lourenco [4] and adapted to ABAQUS as a VUMAT by Haider [5]. This model has the advantage of being specifically developed for masonry, and therefore is based on an orthotropic behavior. Unfortunately, the model is implemented only for plane stress state, and can be used for modeling 2D elements only.

During testing, the in-build DP material model proved to be much more robust, (an important property for such complex 3D model), and therefore has been used for all 3D models. The results obtained with the VUMAT models are partially reported in §3.2.

3.1.1 Unit testing of the two material models

Both proposed material models have been tested under combined in-plane axial and shear loading, in order to evaluate their behavior. The sequential loading scheme used in this testing is presented in Figure 6, and it consisted of (1) a step to load the element with axial stress and (2) then test it in shear while maintaining the existing axial stress value.

Selected result of this testing procedure for the DP and VUMAT material properties are presented in Figure 7. As it can be observed both materials models can sustain significant compression and almost no tension. As mentioned, the DP material model is isotropic; while the VUMAT material model is orthotropic (in this case half the compression capacity in the Y direction has been used in the X direction).

Figure 7 represents the interaction between the 3 stresses, σ-σ-τ. The plots were drawn using the calculated values in distinct points of the σ-σ plane. The red diamond symbols in Figure 7 correspond to calculation points on the margin of the interaction surface in the σ-σ plane (shear stress is $\tau = 0$ in those points); while the cyan circles correspond to proper σ-σ-τ interaction points. Based on the results in the calculation point the isosurfaces in term of τ have been drawn.

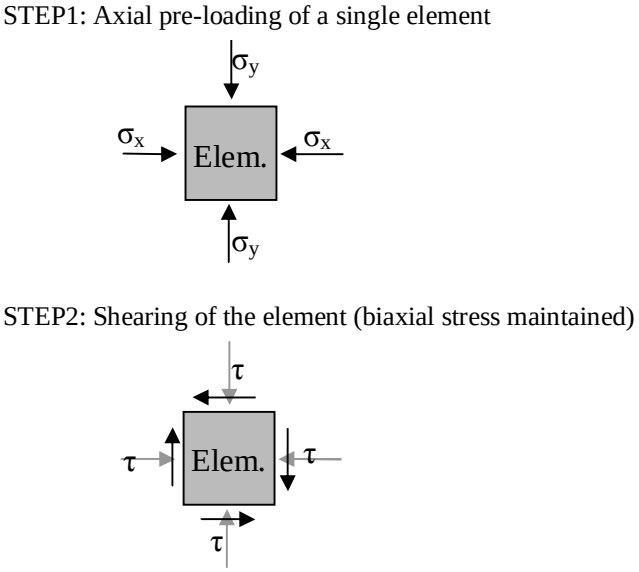

Figure 6. Principle of unit testing of the two material models.

It can be noted that the DP model has a uniaxial compression resistance of 1.5 N/mm^2 [1]. The uniaxial tension capacity in both directions is very small (0.125 N/mm^2), and the maximum shear capacity ($0.6 < \tau < 0.8$ N/mm^2) corresponds to the range of biaxial compression of the magnitude 0.8 N/mm^2. It is also interesting to observe that uniaxial compression is only slightly influences the shear capacity; e.g. at $\sigma_y = 0.8$ and $\sigma_x = 0$ the shear $\tau > 0.2$ N/mm^2. The tendencies are similar in the orthotropic material.

It is important to keep in mind the material interaction surface, as one of the effective ways of improving the behavior of the masonry is to modify the load paths in a way to explore the advantages of this interaction. E.g. one can increase the compressive stress (i.e. locally confine the masonry) in order to increase shear strength.

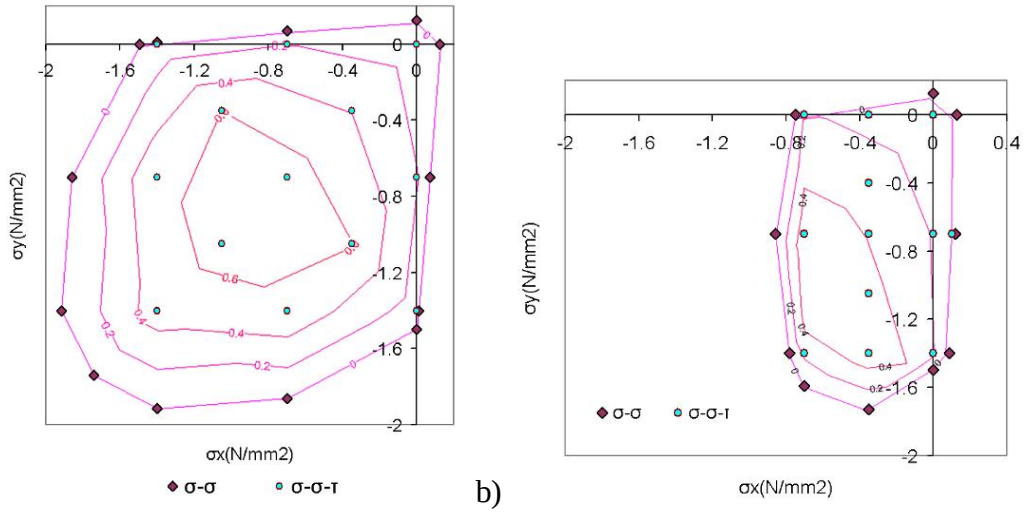

Figure 7. σ-σ-τ interaction of the (a) DP and (b) VUMAT material model.

In the post-failure range, the both the DP material and the VUMAT material are characterized by slow compression degradation dependent on compressive strain, and softening stress-strain response depending on the opening of cracks in tension

(Figure 8). Detailed description of the constitutive models for DP material are in [6], and for the VUMAT material in [4] and [5]. Because the FE model is expected to be used in pushover analysis only, no cyclic damage parameters have been incorporated in the material definition.

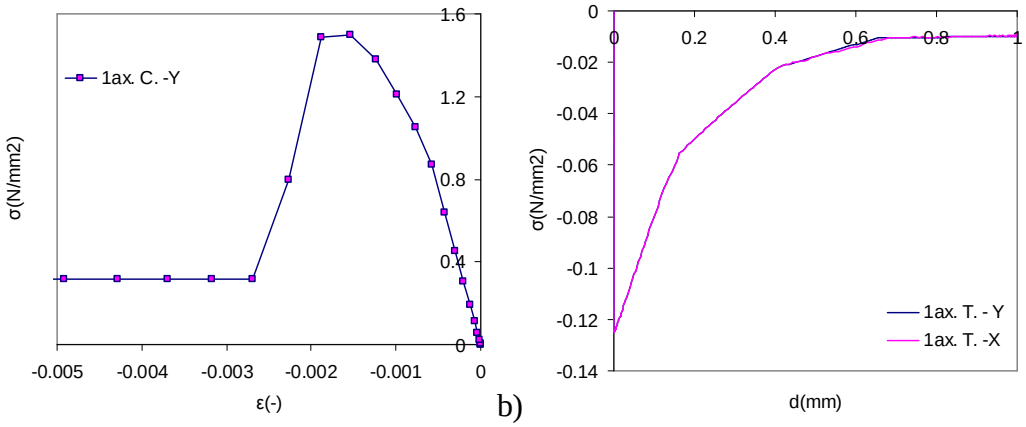

a) b)

Figure 8. (a) Uniaxial compressive and (b) uniaxial tensile behavior of the DP model.

3.2 Testing of 2D wall subassemblies

In the first step, a single wall (i.e. outer wall on the left side of the plan in Figure 1a) was selected and analyzed as plane model. The use of a plane model allowed the direct comparison of the results from the damage plasticity (DP) and the VUMAT models, since the VUMAT model had a plane stress formulation.

The walls were modelled with three support-conditions:

- In the basic case (Case1), the floors were considered rigid and they were forced to move without rotation. I.e. the nodes corresponding to each floor level were slaved to the reference node; hence, their relative position to the reference node was kept constant during the deformation. The reference node was not allowed to rotate. Both horizontal and vertical loads were applied only to the 3 reference nodes, corresponding to the 3 floors.
- In Case2, the floor nodes were connected to the reference nodes, forcing the floor nodes to preserve their relative position during deformation; but the reference nodes were permitted to rotate. Loads were applied as in Case1.
- In Case3, floor nodes were not connected; they were free during deformation. In this case both vertical and horizontal loads were applied distributed to floor nodes.

In the first step vertical loads were applied to the wall at the three floor levels. At each floor level F_V=60kN was applied, and the self weight of the walls was neglected. This load does not correspond to the real loads on the structure; it was chosen by approximation and used for the testing of the model only.

In the second loading step horizontal loads were applied to the nodes corresponding to the floors. The horizontal load at each floor level was proportional to the height of the application point. I.e. this corresponds to triangular load distribution, if the seismic masses are equal at each floor.

The deformation shape of the wall modeled with DP material (at the stage of advanced cracking) is presented in Figure 9, Figure 10 and Figure 11.

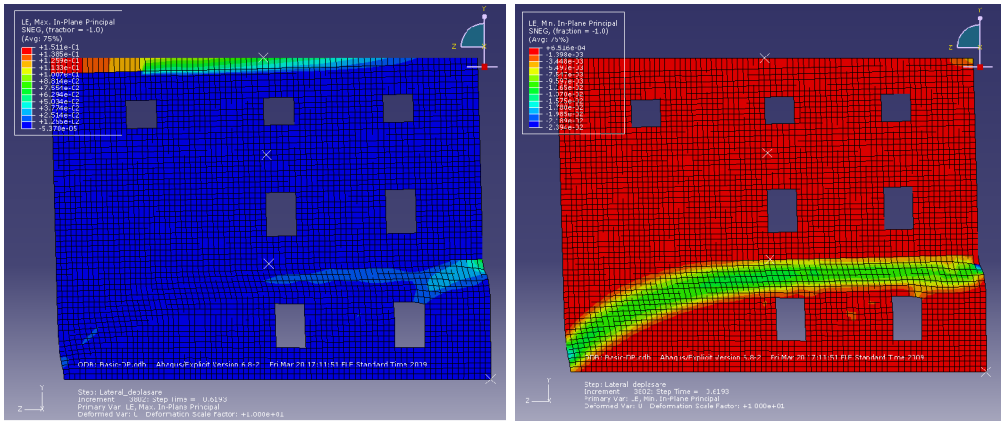

Figure 9. Case1 (Basic-DP) deformation with DP model: (a) plastic strain in tension (b) plastic strain in compression.

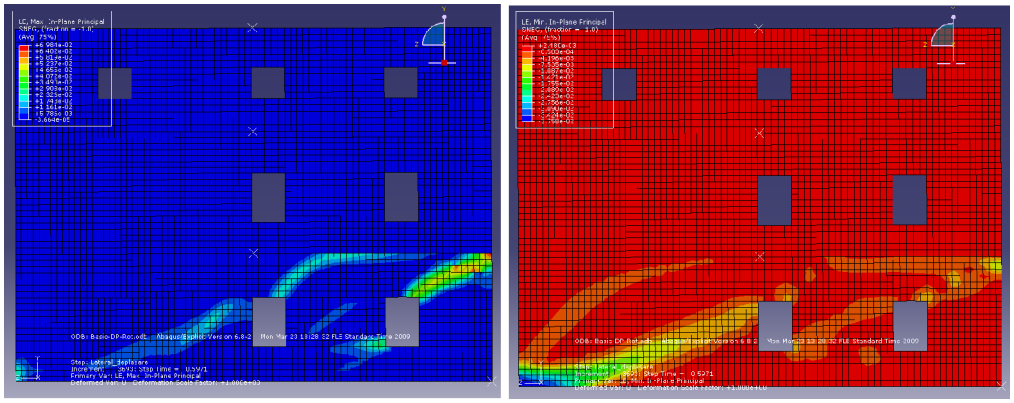

Figure 10. Case2 (Basic-DP-Rot) deformation with DP model: (a) plastic strain in tension (b) plastic strain in compression.

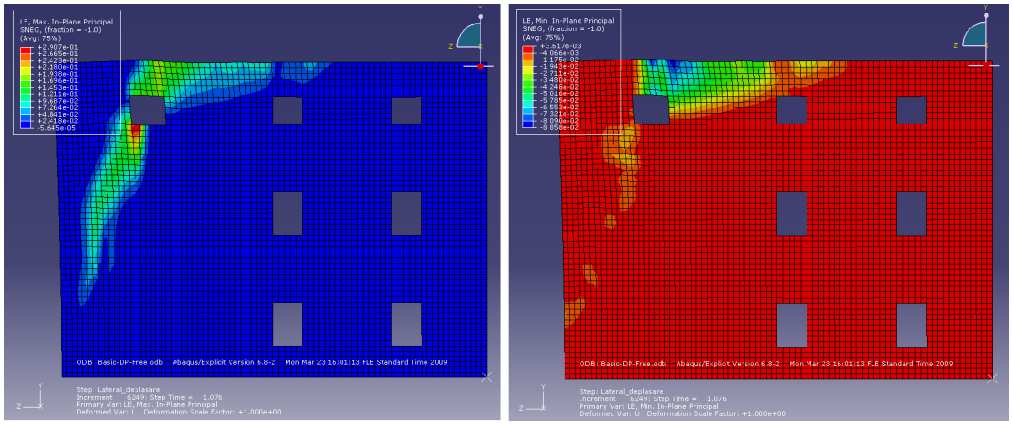

Figure 11. Case3 (Basic-DP-Free) deformation with DP model: (a) plastic strain in tension (b) plastic strain in compression.

As it can be seen, the support conditions at the floors have strong influence on the behavior of the wall. Case1 provides an unrealistic deformation shape as the wall is confined by the enforced horizontal motion of the floor levels. The plastic strains developing in tension (i.e. tension cracking), due to the horizontality moving top floor is clearly impossible in reality (Figure 9a).

Case2 deformation shape appears to be more realistic, and the floor support condition corresponding to this case has been used in further 3D models, when the floor was considered to act as rigid diaphragm.

An interesting, local failure model is developed in Case3. This is possible if the floor does not act as a tie in the plane of the wall. A proper roof diaphragm would eliminate this failure mode, but not because of its in-plane rigidity, but because of the tying effect it provides along the top of the wall. The support and loading condition from Case3 have been used in the further 3D modeling when floor diaphragm was not effective.

Unfortunately all trials to achieve comparative results with the ones from Figure 9, Figure 10 and Figure 11, using the VUMAT material model failed. The wall models using this material model could be loaded with the vertical loads; but obtaining post cracking deformations after the application of the horizontal loads was impossible due to convergence problems. The strains, in the early stage of horizontal load application, can be observed in Figure 12 and Figure 13. Due to the observed convergence problems, the further use of the VUMAT model was renounced.

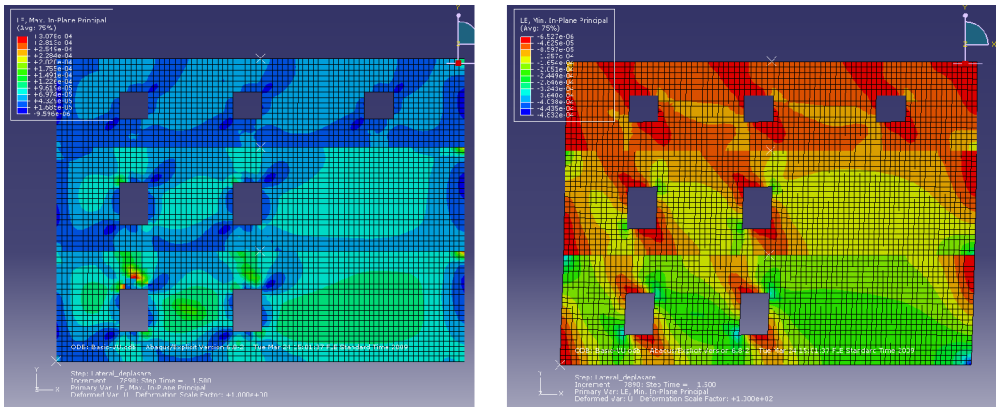

Figure 12. Case1 (Basic-VU) deformation with VUMAT model: (a) plastic strain in tension (b) plastic strain in compression.

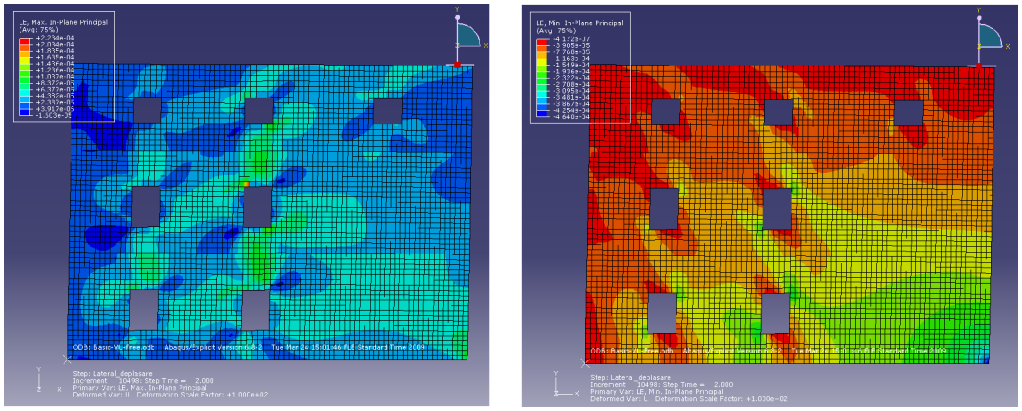

Figure 13. Case3 (Basic-VU-Free) deformation with VUMAT model: (a) plastic strain in tension (b) plastic strain in compression.

The force displacement curves from the five wall models discussed above is presented in Figure 14. As it can be seen from Figure 14a, the vertical uploading of all models is very similar. Once the total vertical load level of 180kN has been

reached, the force level is kept constant, even if the top node can still undergo displacements as the horizontal loading is applied, in the next step.

From the curves in Figure 14b, corresponding to the horizontal loading (i.e. pushover analysis), it can be concluded, that the initial stiffness of all models is similar. This is encouraging as the DP and the VUMAT models have different source (i.e. DP is in-build to ABAQUS, while VUMAT is from an external subroutine); and by this correspondence they increase the confidence in the results.

Furthermore, the curve of the Basic-VU model (i.e. Case1 with VUMAT material) follows the Basic-DP model (i.e. Case1 with DP material) curve up until the onset of cracking. Therefore, the two material models predict the same cracking load for the Case1 walls, leaving in doubt only the levels of ductility predicted by the DP material model, which could not be replicated with the VUMAT model.

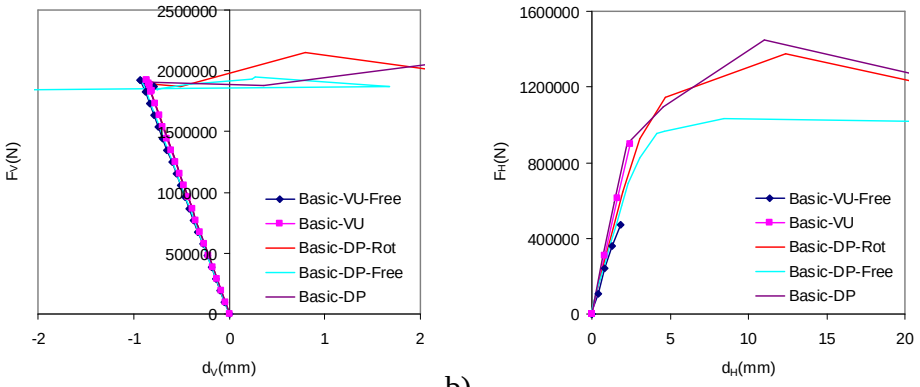

a) b)

Figure 14. Load displacement curves for the wall models: (a) vertical load vs. top vertical displacement, (b) base shear vs. top horizontal displacement

3.3 Loading methodology of the 3D model

In the next modeling step, the full 3D model of the masonry house has been tested considering different techniques of load transmission. Vertical loads, according to the distribution presented in Table 1, and horizontal loads according to the distribution from Table 2, were transmitted to the 3D model in two ways. In both cases, the self weight of the masonry walls was modelled by taking into account the density of the material and the gravitational acceleration (i.e. the mass of the walls was distributed in the volume of the walls). The two loading techniques were different only in the respect of transmitting the vertical floor loads and horizontal pushover loads.

In the firsts case (i.e. rigid floor models) the floors were considered to behave like “rigid body” (i.e. all 3 displacements of the floor nodes were constrained to remain in the same relative position after deformation as they were before deformation). This scheme of modeling the floor is the 3D equivalent of the technique used in Case2 for the 2D walls (Figure 10). Both vertical and horizontal forces have been applied as concentrated force in the centre of mass of the rigid body. One example for the constraint and vertical force of the top floor is given in Figure 15.

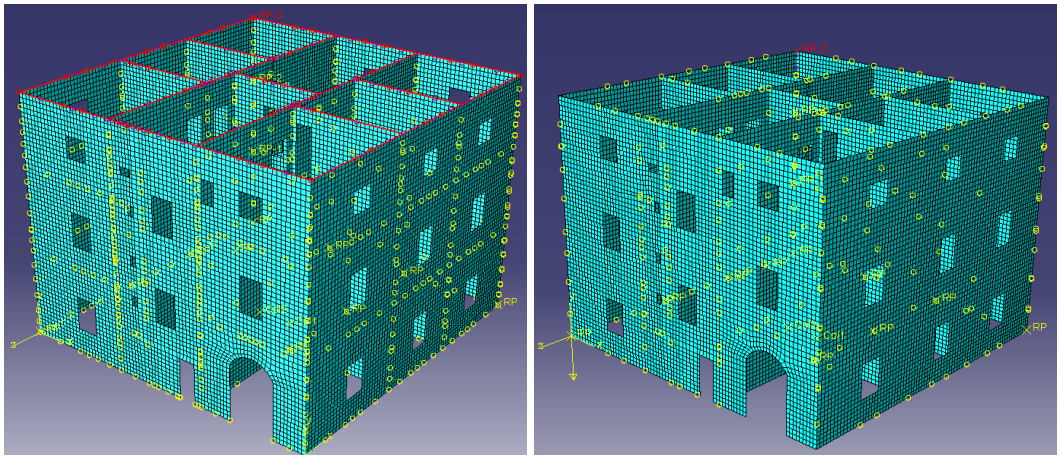

Figure 15. "(a) Rigid body" constraint on nodes of the upper floor & (b) concentrated load applied to the reference point of the "rigid-body".

In the second case the floors were neglected and vertical and horizontal loads have been uniformly distributed on all nodes of the floor (i.e. floor free models). This modeling techniques is the 3D equivalent of the Case3 modeling scheme for the 2D walls (Figure 11). The loading scheme is presented in Figure 16.

Both of the above techniques of modeling the vertical loads can be criticized. The "rigid body" modeling of the floors is not correct because it creates floors which are infinitely rigid in out of plane bending. This is not true for real floors and it goes beyond the "rigid diaphragm" requirement formulated by the design codes, e.g. EN 1998 [7]. The distribution of floor loads equally to every node on the perimeter of the floor level is also not correct, because in reality forces are distributed according to the tributary areas on the floor supported by each wall segment. However, the simplifications for floor modeling and load distribution have been accepted as a means of simplifying the model.

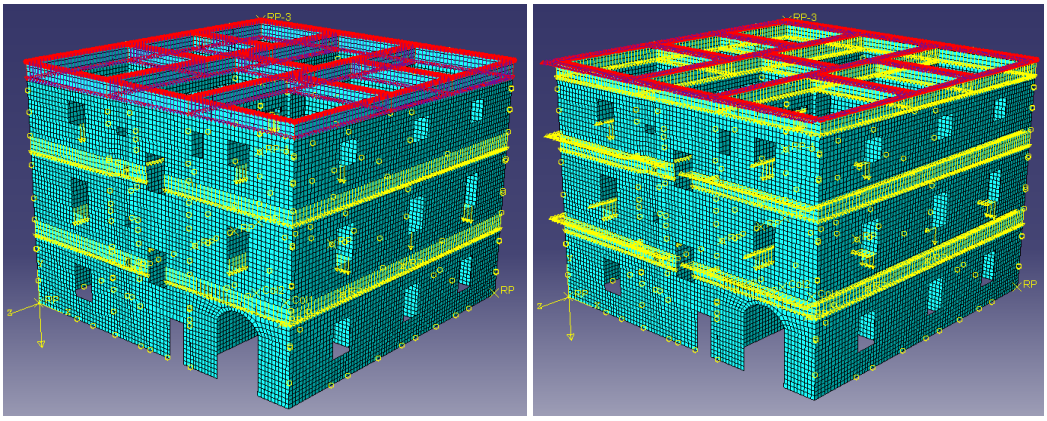

Figure 16. Floor free model loaded with (a) vertical load and (b) horizontal load on the top floor.

4 Initial assessment of the building

4.1 Vertical loads

Under the vertical loads corresponding to the earthquake load combination, the masonry walls will develop a stress pattern, which will affect the performance to horizontal pushover. As shown in Figure 7, there is a strong interaction between the normal and shear stresses in the masonry material. The stress state under vertical loads is presented in Figure 17.a for the *rigid floor* and in Figure 17.b for the *floor free* model.

As it can be seen in Figure 17 the largest compression stress, corresponding to σ_y in Figure 7, is -0.47N/mm^2 and -0.57 N/mm^2 respectively. This means 30% from 1.5 N/mm^2, corresponding to uniaxial compressive failure stress of the masonry.

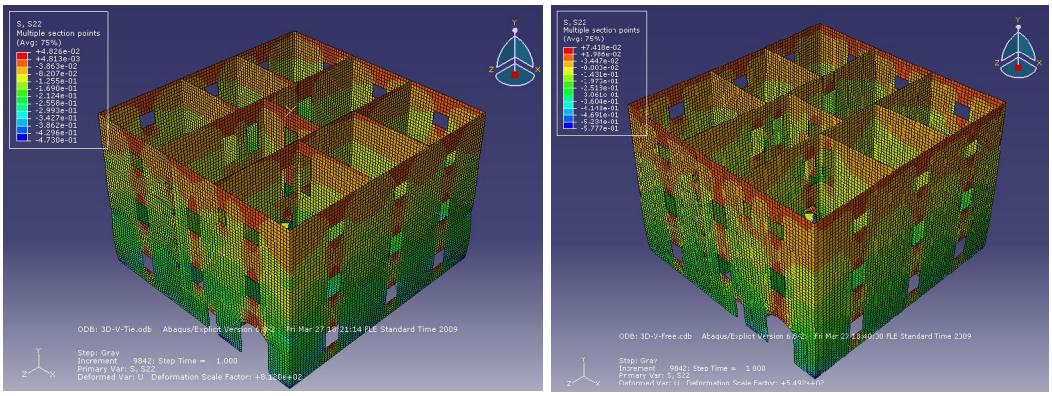

(a) (b)

Figure 17. 2-2 (Y-Y) direction stresses in the masonry from vertical loads.

The load vs. vertical displacement curves are also presented for the two models in Figure 18. It can be observed that the model using “rigid floor” assumption is slightly stiffer, but no significant difference has been observed. This is probably caused by the fact that 74% of the vertical load is the mass of the walls (see Table 1), so the distribution of the remaining 26% load is not crucial.

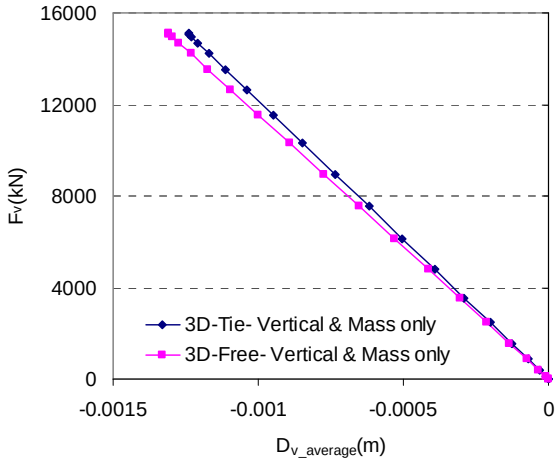

Figure 18. Vertical load vs. vertical displacement.

4.2 Horizontal loads

4.2.1 “Floor-free” configuration

Given the way floors are constructed, the original building can be considered as floor free, because the existing floor arrangements ensure very limited diaphragm action. If the 3D, floor free model is analyzed steadily increasing horizontal forces, the deformed shape presented in Figure 19 is obtained.

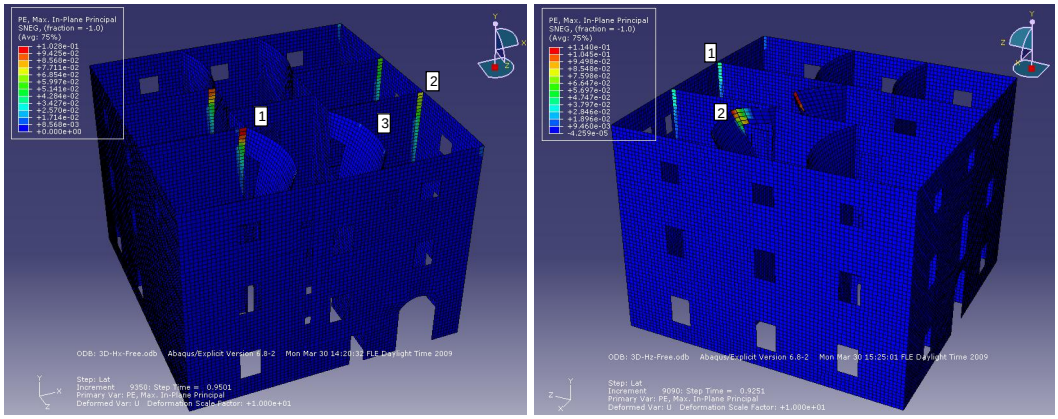

Figure 19. Plastic-strain/cracking pattern at failure for (a) X direction and (b) Z direction pushover.

It can be observed that, under this pushover type loading, the failure mode of the structure is always based on a local mechanism. One main failure mode is due to the separation of the heavy external walls from the transversal ones (e.g. Point 2 in Figure 19a). The second failure mode is by out of plane deformation of wall segments perpendicular to the loading direction (e.g. Point 3 in Figure 19a). As it can be observed in Figure 20, both phenomena happens at a very small value of the base shear, below and around F_b = 800 kN. Keeping in mind that the order of magnitude of the base shear is expected to be in the range of thousands (e.g. 8900 kN is the order of magnitude discussed in §2.3.3) it appear that one o the goals of the rehabilitation will have to be the tying together of the walls, in order to avoid localized failure modes.

Possibly, it may be necessary to establish diaphragm effect at each floor level within the structure, in order to ensure more uniform distribution of the stresses and cracking under the horizontal loads.

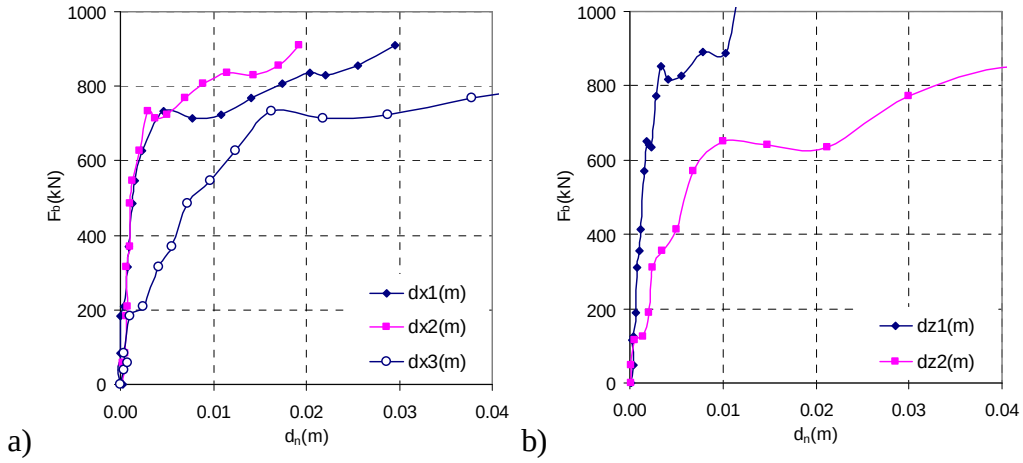

Figure 20. Deformations in the points of Figure 19 vs. the base shear in (a) X direction and (b) Z direction loading.

4.2.2 Rigid body floor configuration

The most realistic estimation of the current state of the structure is to presume zero diaphragm effect. This model has been explored in the previous chapter. On the other hand, the largest improvement to be done to the structure, without modifying the walls, is to establish diaphragm action at each floor level. This is the "upper bound" of what can be achieved without improving the vertical load bearing system (i.e the walls). The FE model simulating full "rigid body" floors has been analyzed under similar pushover loads as the previous "floor free" model. The deformed shape of the model under X and Z direction loads is presented in Figure 21.

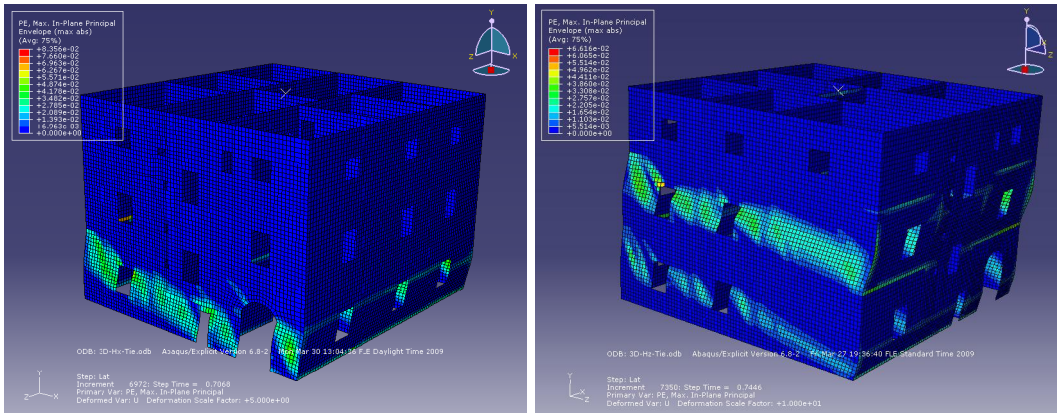

Figure 21. Plastic strain for (a) X and (b) Z direction pushover of rigid floor model.

The pushover curves in the two directions are presented in Figure 22. In fact the base shear force is given both in the direction of loading (Fbx-X & Fbz-Z) and perpendicularly to the loading direction (Fbx-Z & Fbz-X). As it can be observed in Figure 22, the perpendicular direction base shear is very small compared to the loading direction base shear. This shows that, even if the structure is not symmetrical, there is not much interaction due to torsion. In case of a more unsymmetrical structure, such torsion effects can be significant, and walls perpendicular to loading/pushing direction can also be loaded. As reported by Kilar and Fajfar [9], in strongly unsymmetrical buildings, load bearing walls or

frames perpendicular to the loading direction can even develop failure and be the limiting factor of the overall performance.

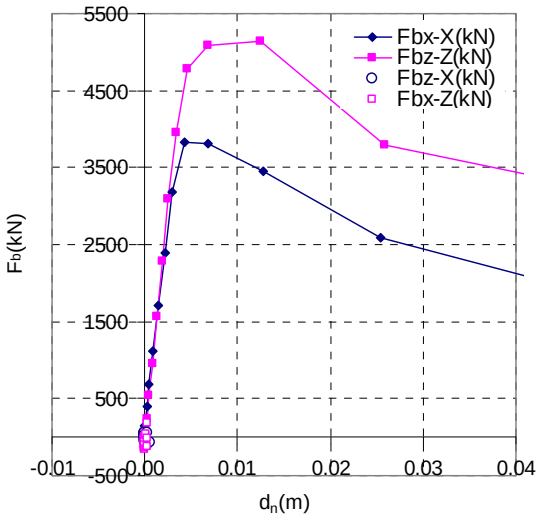

Figure 22. Pushover curve in case of X and Z direction loading.

If the pushover curves from Figure 22 are transformed in PSA-SD format using the elastic spectra with the design PGA level, the plots in Figure 23 are obtained. As it can be seen, the structure has a satisfactory performance in the Z direction, and underperforms in the X direction. In the Z direction, the structure is both strong (91% of the elastic requirement) and sufficiently ductile ($\mu = 2.6$). In the X direction however, the structure is weaker (68% of the elastic demand). But what is worst, it is also less ductile (μ can hardly be defined). In both directions, the structure is very stiff, with an equivalent SDOF period of vibration of $T^* = 0.16$ s.

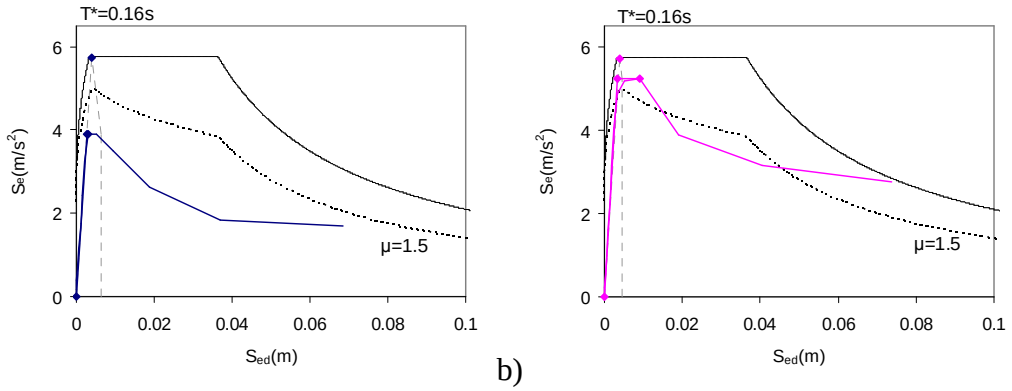

Figure 23. PSA-SD plot vs. pushover curve transformed in SDOF format (a) X & (b) Z direction.

The results presented in Figure 23 are based on the standard mass distribution shown in Figure 3a. One interesting conclusion of the preliminary analysis was that, if the alternative mass distribution is used (Figure 3a), the results of the pushover analysis are rather different. As illustrated in Figure 24a, deformation in the Z direction is changed from a global failure into a ground-floor/soft-storey mechanism. As shown in Figure 24b, this change has an important impact on the ductility of the structure in the Z direction. Behavior in the X direction however is not affected (Figure 24b).

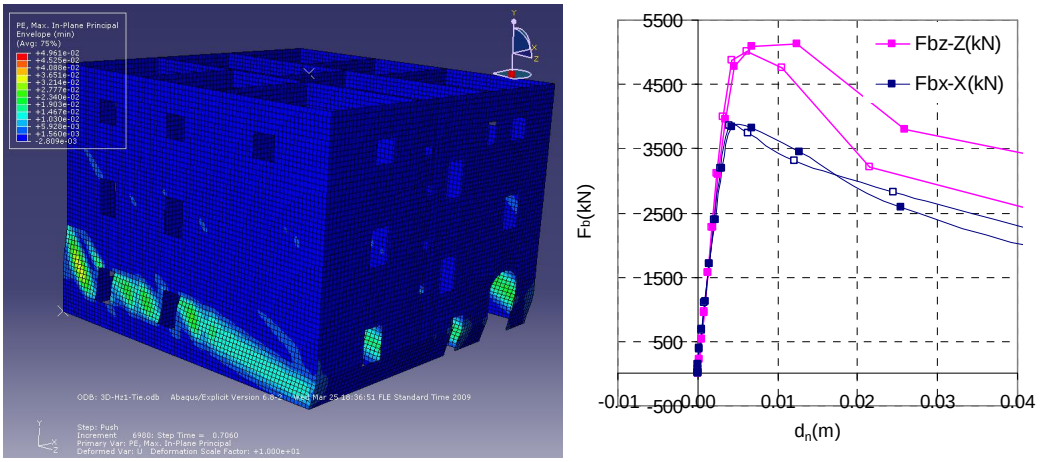

Figure 24. (a) Z deformation using the alternative mass distribution and (b) comparative pushover curves.

This comparison is highlighted in this report in order to illustrate the sensitivity of the modeling to load distribution, especially as far as ductility is concerned.

4.3 Deficiencies of the existing building

As far as the current configuration is concerned the following structural properties and potential deficiencies have been identified:

- The structure is almost symmetrical and has similar behavior in the two main directions. Torsion does not affect the performance.
- The largest part of the seismic mass is given by the weight of the wall elements. Both the weight of the floors and the mass coming from live load is less significant.
- In the current configuration the biggest weakness of the structure is the lack of diaphragm effect at both the level of the floors and at the level of the roof. As consequence the walls are not tied together and local failure is governing the behavior. Realizing an effective tying between the walls has to be the main priority of any rehabilitation.
- If floor diaphragm action is realized the structure would have satisfactory performance in the Z direction. However in the Z direction supplementary intervention is most probably required.

4.4 Discussion on the possible use of LGS for the rehabilitation

It is clear from Table 3 that the structure has a very high value of seismic mass. On the other hand, if 3D box like behavior is ensured (e.g. by providing diaphragm at floor levels) the building is very rigid. In both directions, the fundamental period of vibration is evaluated to be T=0.16s (Figure 22).

In these conditions, the use of LGS as rehabilitation material is limited due to the following factors:

- The strength of an LGS system (e.g. frame of shear wall), placed in parallel to the existing structure can not provide sufficient strength to resist horizontal forces generated by such large seismic masses.
- Parallel load bearing LGS systems can not achieve sufficient stiffness to be activated at the deformation levels developed by the masonry.

This means that, once diaphragm action is achieved, the masonry walls can not be strengthened by parallel load bearing LGS systems. LGS has potential use for this structure as:

- Strengthening elements in order to achieve 3D box like behavior. E.g. roof diaphragm can be realized with a plane truss system placed at the top of the walls. This truss system can be made from hot-rolled or from LGS profiles.
- Elements to achieve diaphragm action at the level of each floor. E.g. horizontal trusses made of LGS can be placed in each room, connected to the existing floor and to the walls, in order to stiffen and strengthen the in plane response of the floors. LGS has the particular advantage of easy handling in the confined spaces. LGS members should be used as elements of a truss (i.e. working in axial direction), and not as bending members. In bending their high flexibility, makes the LGS profiles inefficient in participating in the load transmission.
- Strengthening members for floors in the vertical direction, e.g. by supplementing or replacing timber floor beams. (This is not strictly an intervention in case of earthquake and it is not discussed in this document).

One technique is suggested for the use of LGS to strengthen the masonry itself. In this case the LGS is resisting the horizontal loads not as a parallel system with the masonry, but instead it is imbedded in the masonry itself, enhancing its properties (i.e. tensile strength). It is suggested that this can be achieved by gluing-in narrow LGS strips in precut horizontal slots (Figure 30).

The solution is similar to the use of reinforcement in reinforced-masonry walls (Figure 25), and it is expected to have the same benefits.

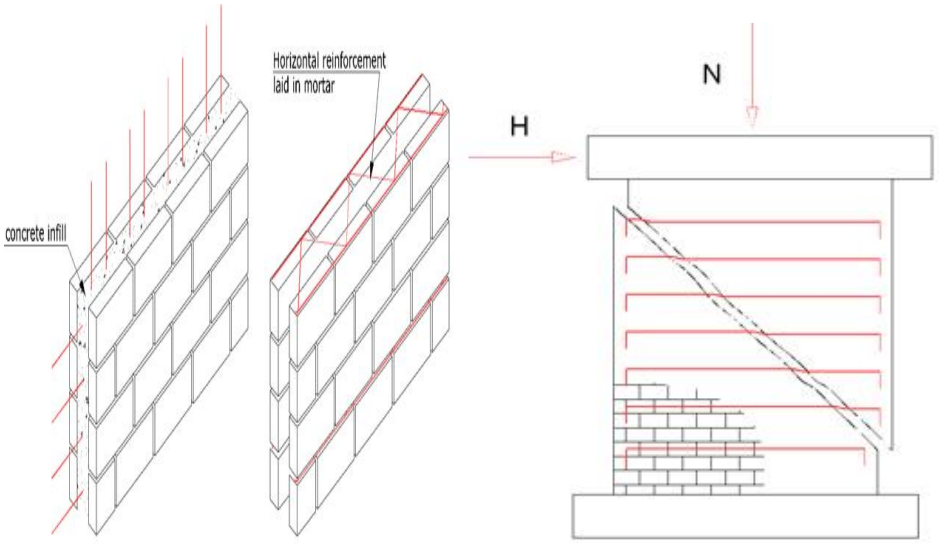

Figure 25. Reinforced masonry and expected failure mechanism of wall loaded by horizontal load [10]

5 Proposed rehabilitation methods

Based on the observations concerning the behavior of the structure the following rehabilitation techniques have been tested:

- Tying of the upper part of the walls, using tension only ties.
- Establishing rigid diaphragm at the top of the walls.
- Rigid diaphragm at roof level, coupled with reinforcement of the external ground floor walls with horizontal LGS strips.
- Rigid diaphragm at each floor level, coupled with reinforcement of external ground floor walls with horizontal LGS strips.

5.1 Tying the top of walls

As mentioned earlier one of the weaknesses of the structure is that walls are not tied, and they have the tendency to separate (Figure 19). Therefore the first rehabilitation solution proposes the full tying of the upper end of the walls, but without realizing diaphragm effect. Figure 26 presents the deformed shape of the structure, under distributed push-over loads, when the top of the walls have been tied using Φ24 mm, f_y = 350 N/mm^2 steel bars.

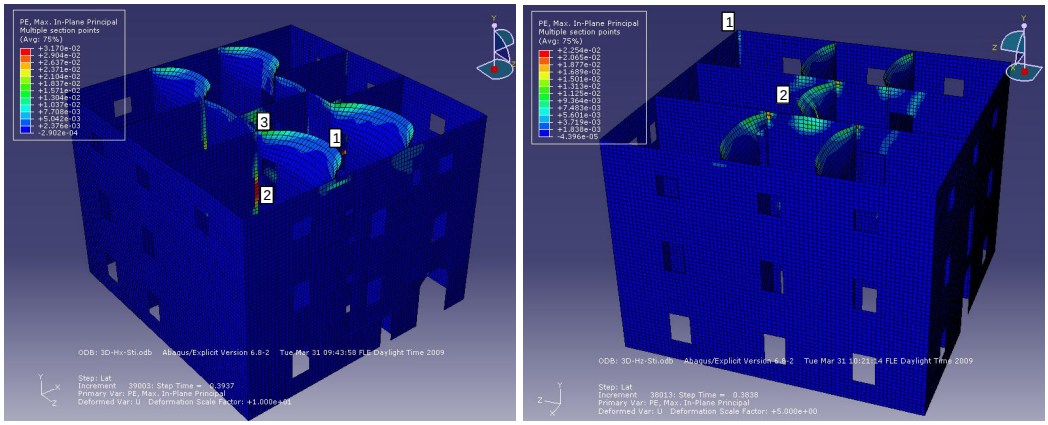

(a) (b)

Figure 26. Pushover deformations with Φ24 mm, f_y = 350 N/mm^2 tying at the top of the walls.

As it can be observed, tying solves part of the problems of the structure, namely, separation of the walls at vertical connections is mostly eliminated. Some tendency of separation (i.e. tension cracking) can still be observed at the X direction push-over, at the height of the second floor slab (Point 2 on Figure 26a). This indicates that tying should be done not only at the top of the walls, but also at intermediate levels, in order to completely eliminate the tendency of separation.

A remaining problem of the structure is the out of plane bending of walls, which was not eliminated by the tying. The pushover curves using this configuration are presented in Figure 27. It can be noted that base shear force has approximately doubled compared to the curves from Figure 20. It appears that the only technique in order to eliminate out/of plane failure of the walls is to introduce bending stiffness at the mid-span of the walls.

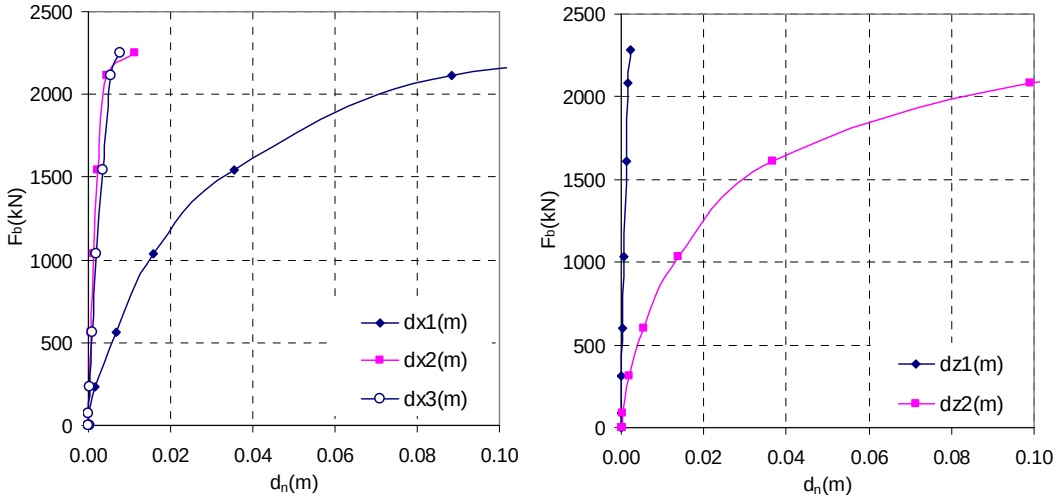

(a) (b)

Figure 27. Pushover curves of structure tied at top with Φ24 mm, f_y = 350 N/mm^2 ties. (a) X (b) Z direction.

5.2 Rigid diaphragm at the roof level

The level of rehabilitation could be not only to provide tying, but to establish diaphragm action at the top of the walls. This, of course, is both more technically challenging and more expensive procedure compared to tying; and it supposes the realization of a r.c. slab or a horizontal steel truss system at the top of the walls.

This case has been modeled in ABAQUS by providing a “rigid body” constraint for nodes at the top of the walls. Deformation shape under push-over loading is presented in Figure 28. As it can be observed the cracking of the walls is uniformly distributed over large areas, which is definitely an advantage of the solution. However, localized failures are still present: (i) separation of vertical wall connection at the level of the second slab (Figure 28a2) and, (ii) out of plane failure of an entire wall at the second floor level (Figure 28b2). Supplementary local intervention and strengthening, besides the roof diaphragm, is required to eliminate these failure modes.

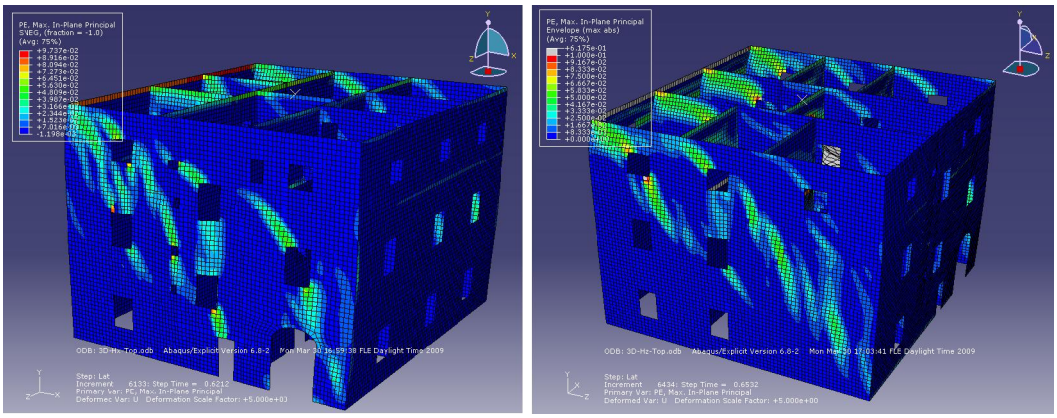

(a-1) (b-1)

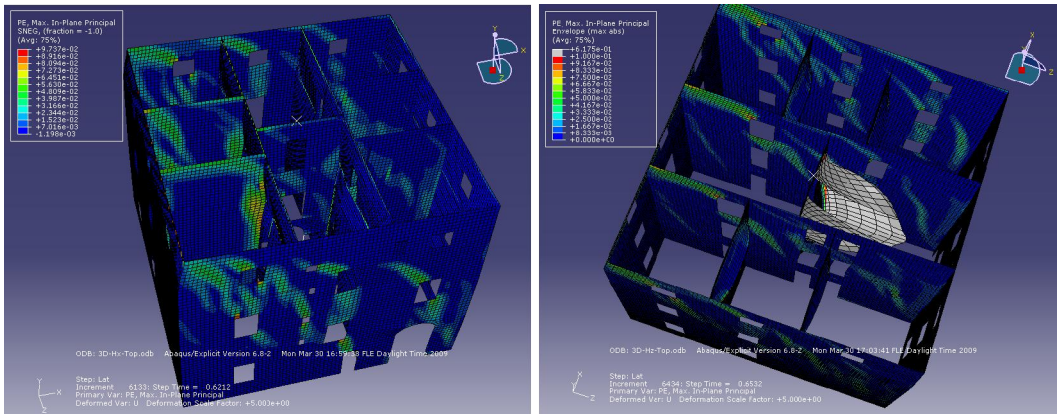

(a-2) (b-2)

Figure 28. Views of the deformed shape and distribution of tension cracking for (a) X and (b) Z direction pushover.

The overall performance of the structure is very advantageous in this configuration. As one can observe from the curves in Figure 29, the rehabilitated structure possesses sufficient strength and ductility to withstand the design earthquake load in both X and Z direction. As it can be observed from comparing Figure 29 with Figure 23, this rehabilitation method providing less strength but substantially more ductility, compared to the one involving rigid diaphragm at each floor level. Also, the disadvantageous soft/storey failure mode, observed in Figure 19 is avoided.

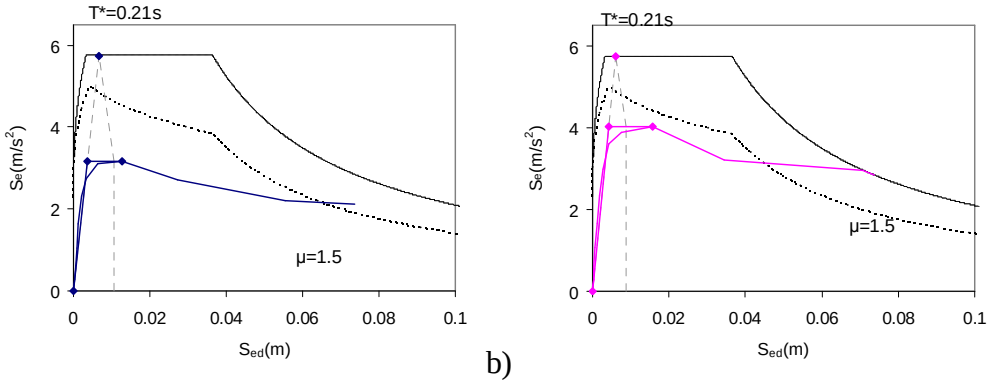

a) b)

Figure 29. PSA-SD plot vs. pushover curve transformed in SDOF format (a) X & (b) Z direction.

5.3 Rigid diaphragm at roof level - LGS strips for external walls at ground floor

Even though the previously presented rehabilitation technique is sufficient to fulfill the earthquake design requirements, it has been decided to try to further improve the properties of the building by strengthening selected walls with horizontal LGS steel strips. The proposed technical solution is presented in Figure 30, and it involves the gluing of steel strips (A_{strip} = 20 mm^2) in pre-cut slots of 50 mm depth. The slots are supposed to be cut at 200 mm intervals. This proposal is inspired from the so called surface-mounted FRP solutions, frequently used for masonry strengthening; but it is hoped that the steel strips would have better performance due to the larger elastic modulus of steel compared to FRP.

Therefore, at small strains larger loads could be transmitted to the reinforcing strips.

The logic of placing the strips horizontally is illustrated in Figure 30b. It is expected that the interaction between the masonry and strips will provide additional tension strength in the X direction. Therefore, the initial isoshear surfaces (i.e. magenta lines in Figure 30b, reproduced from Figure 7) will be extended in the positive direction of the X axis (i.e. dashed blur lines in Figure 30b), and the shear strength of the masonry will be increased. This solution is explored in this report as a possibility; to test the efficiency of such LGS steel solution both further theoretical study and testing would be necessary.

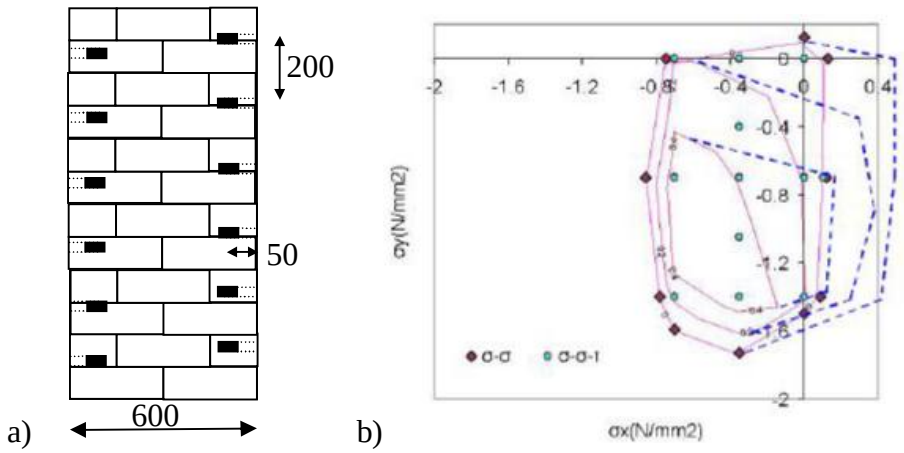

Figure 30. (a) Technical solution for horizontal LGS strips and (b) expected working principle.

From the FEM point of view, the implementation of the LGS strip reinforcements is straightforward in ABAQUS, as reinforcement of the existing shells. The strengthening with LGS has been applied only to ground floor external walls, with a thickness of 60 mm. Similar push-over analyses, as in the previous cases, has been carried out, and the deformation shapes of the structure are presented in that Figure 31. If one compares Figure 31a with Figure 28a1, and Figure 31b with Figure 28b1, it is clear that tensile cracking is reduced in the ground floor walls when LGS strengthening is used.

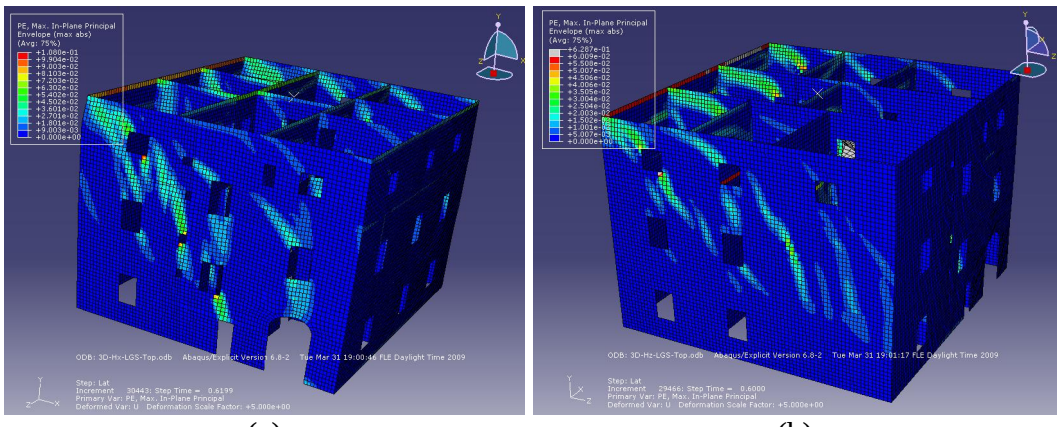

(a) (b)

Figure 31. Deformation shapes and distribution of tension cracks for LGS model. (a) X direction and (b) Z direction pushover.

The push-over curves from the structure without, and with LGS strengthening, are compared in Figure 32. It is clear from the figure that, even if the cracking pattern is slightly modified, the overall performance of the building has not been fundamentally changed by the LGS strengthening. In order to have a performance improvement, the LGS strips should probably be extended all the way up to the roof slab, where they can interact with the rigid diaphragm.

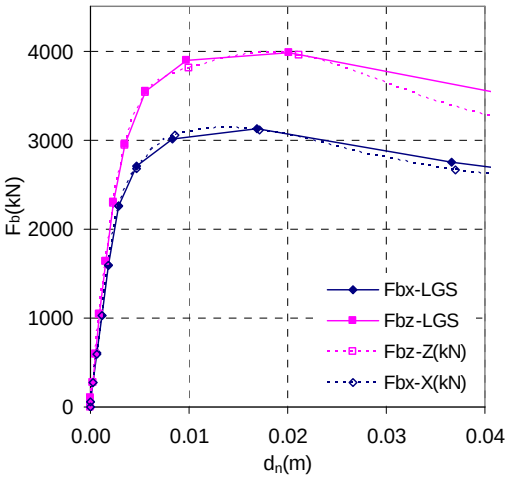

Figure 32. Comparison of pushover curves without and with LGS strengthening of selected external walls, diaphragm provided only at roof level.

5.4 Rigid diaphragm at each floor - LGS strips for external walls at ground floor

Finally, an attempt to combining the LGS strips with rigid diaphragm at each floor level has been made. As previously, LGS strips have been applied only to ground floor external walls. The deformed shape and the tensile cracking pattern from pushover loads, in the X and Z directions, are presented in Figure 33. The most notable difference between this deformation shapes, and the ones presented in Figure 21 (i.e. same structure but without LGS strengthening), is that, under Z direction forces the initial two-floor mechanism (Figure 21b) has changed into a single floor mechanism on the second floor (Figure 33b). This is caused by the gain of strength of the ground floor caused by the LGS strengthening.

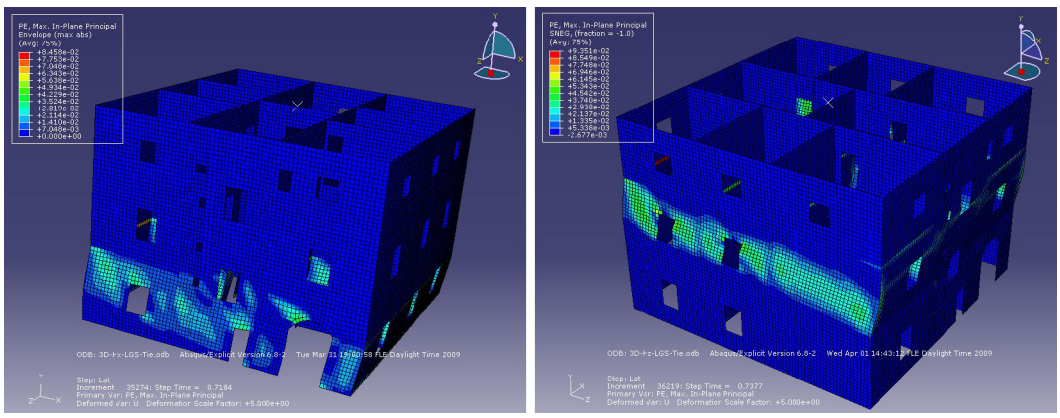

(a) (b)

Figure 33. Deformed shape and tensile cracking pattern for (a) X and (b) Z direction pushover.

The comparative push-over curves, from the structure without and with LGS strengthening are presented in Figure 34. As it can be observed, the effect of the LGS strengthening is more significant then in the case presented in Figure 32. A measurable improvement of the performance can be observed both in terms of strength and ductility, especially in the X loading direction. Based on these results, it can be appreciated that using LGS strips, in the presented configuration can bring benefits to the performance of masonry structures, if the strengthening is well distributed.

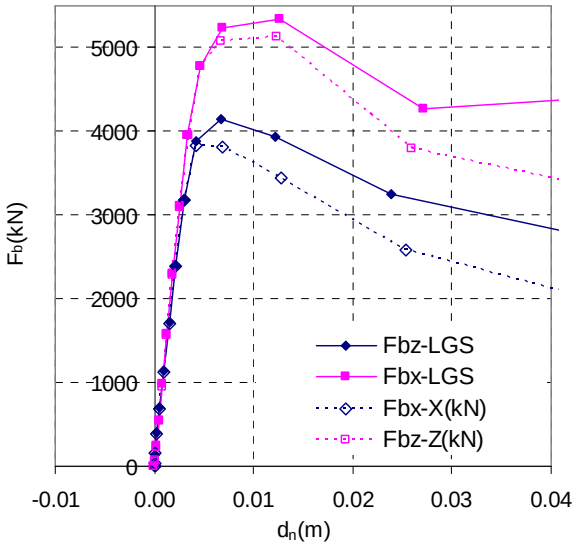

Figure 34. Comparison of pushover curves without and with LGS strengthening of selected external walls (i.e. diaphragm provided only at each slab).

6 Conclusions

In this document non-linear modeling techniques have been explored for the evaluation of the performance of the masonry benchmarks structure within the STEELRETRO project. ABAQUS has been utilized as the main modeling tool for the work presented.

Two alternative modeling techniques of the masonry material have been used: (i) one based on the in-build concrete damage-plasticity (DP) model of ABAQUS and, (ii) and the second based on the use of an external VUMAT subroutine. As the DP material definition has proved both more flexible and more stable, this model has been mainly used. However, it is noted that the main disadvantage of the DP material model is its inability to take into account orthotropic behavior of the masonry.

For the evaluation of the earthquake performance of the benchmark masonry structure, classical, pushover analyses has been used. An initial analysis of the structure highlighted that the main weaknesses of the building are: (i) the weak connections between walls and (ii) a low out-of-plane bending strength of the walls. It was determined that the tying together of the walls has to be the priority of any intervention to improve earthquake performance. Further improvement could be obtained if rigid diaphragm was provided at the level of slabs. As a last resort the walls could also be strengthened to increase their lateral load bearing capacity, and a possible technique was presented based on the use of LGS strips.

Five rehabilitation techniques have been proposed, analyzed and reported. The summary of their performance is presented in Table 4.

Table 4. Performance of the 5 intervention techniques tested on the structure.

Nr.	Inadequate/deficient response of the structure	Cause of the deficient response	Intervention technique									
			Tying wall tops with Φ24 mm, f_y = 350 N/mm^2 steel rods		Roof level diaphragm		Diaphragm at each floor		LGS strips + roof level diaphragm		LGS strips + roof diaphragm	
			Obj.	Sol.?	Obj.	Sol.?	Obj.	Sol.?	Obj.	Sol.?	Obj.	Sol.?
1	”Unzipping” of transversal walls (X direction);	No connection at vertical seam	Main	Yes	Main	Partially	Main	Yes	Main	Yes	Main	Yes
2	“Unzipping” of transversal walls (Z direction);	No connection at vertical seam	Main	Yes	Main	Yes	Main	Yes	Main	Yes	Main	Yes
3	Out of plane failure of transversal walls (X direction).	Low bending resistance	Yes	No	Main	Yes	Main	Yes	Main	No	Main	Yes
4	Out of plane failure of transversal walls (Z direction	Low bending resistance	Yes	No	Main	Partially	Main	Yes	Main	No	Main	Yes
5	Soft-storey ground floor mechanism X direction	-	-	-	-	Yes	-	No	-	-	-	No
6	Potential soft storey mechanism in Z direction	-	-	-	-	Yes	-	No	-	-		No
7	Low ductility in X direction	-	-	-	-	Yes	-	No	Yes	No	Yes	No
8	Low ductility in Z direction	-	-	-	-	Yes	-	No	Yes	No	Yes	No
	Overall assessment of the technique		Fail		OK		Fail		OK		OK	

Notes: Obj. - Is it the objective of the intervention technique to correct this deficiency? Respond “Main” if it is the main objective of the intervention. Respond “Yes” if it addresses the deficiency, but it was not the primary purpose of the intervention.

Sol.? - Does the intervention solve deficiency of the structure? “Yes” if it does, “No” if it does not. In some cases the intervention partially solves the problem & other local strengthening would be required.

As it can be observed (Table 4), the tying together of the top of the walls only partially solves the deficiencies of the structure. Separation of wall segments is eliminated; but out of plane bending remains a weakness. For this solution it is improper to speak about global behavior of the structure, as performance is limited by local, out-of-plane failure of the walls. In this particular case, while the tying solution improves the performance of the building, it fails to improve it sufficiently in order to fulfill the designed criteria for a PGA of 0.24 g.

The introduction of a rigid diaphragm at some slab levels clearly change the behavior of the building, from one dominated by local failures, into one governed by global failure. One can speak now about the global performance of the structure. It has been found that introducing rigid diaphragm only at roof level brings more benefits than rigid diaphragms at each slab (Table 4). This is essentially because the presence of only a roof diaphragm forces the structure to behave as a whole; cracking is evenly distributed on the full height of the walls, the formation of soft-storey mechanism is eliminated and the global ductility is superior. On the contrary, the presence of rigid diaphragms at each floor level increases the chance of localized cracking of the masonry, therefore reducing the overall ductility of the structure (Figure 23 vs. Figure 29).

Besides providing rigid diaphragm at slab levels, the improvement of the structure by strengthening the masonry walls themselves is also possible. The possible use of horizontal LGS strips, glued in the masonry, has been investigated for this

purpose. This technique is a steel replica of the FRP based “near surface-mounted” reinforcement solution. Even if it seems to be beneficial from the global performance point of view (Table 4), it has to be noted that this solution needs substantial future investigation (including testing) before it can be claimed beneficial.

References

[1] Braconi, A., Osta, A., Nardini, L., Salvatore, W. "Definition of the masonry benchmark building for the execution of comparative performance analysis between steel intervention techniques." University of Pisa, RIVA Acciaio SpA, 2008.

[2] Varelis, G., Vasilikis, D., Karamanos, S., and Tsintzos P. "Masonry Benchmark Structure." University of Thessaly, Shelter S.A., 2009.

[3] Dogariu A. Proposal for the 3D modeling of the benchmark structure - Frankfurt 11.01.2009 Work meeting.

[4] Lourenco, P. "Computational strategies for masonry structures." Delft: Delft University, 1996. (PhD. Thesis)

[5] Haider, W. "Inplane response of wide spaced reinforced masonry shear walls." Central Queensland University, Australia, 2007. (PhD Thesis)

[6] "ABAQUS 6.8 Documentation, DS Simulia."

[7] EN1998-1. "Eurocode 8: Design of structures for earthquake resistance. Part 1: General rules, seismic actions and rules for buildings." Brussels: European Committee for Standardization, 2005.

[8] prEN1990. "Eurocode - Basis of structural design." Brussels: European Committee for Standardization, 2001.

[9] Kilar, V., and Fajfar, P. "Simple push-over analysis of asymmetric buildings." Earthquake Engineering and Structural Dynamics 26 (1997): 233 - 249.

[10] http://www.staff.city.ac.uk/earthquakes/MasonryBrick/ReinforcedBrickMasonry.htm